The impact of small adsorbates in the vibrational spectra of Mg- and Zn-MOF-74 revealed by first-principles calculations

Carlos Romero-Muñiz,[*,†] José María Gavira-Vallejo,[‡] Patrick J. Merkling,[†] and Sofía Calero[*,†,¶]

†*Department of Physical, Chemical and Natural Systems, Universidad Pablo de Olavide, Ctra. Utrera Km. 1, E-41013, Seville, Spain.*

‡*Departamento de Ciencias y Técnicas Fisicoquímicas, Facultad de Ciencias, Universidad Nacional de Educación a Distancia (UNED), Paseo de la Senda del Rey 9, E-28040 Madrid, Spain*

¶*Materials Simulation & Modelling, Department of Applied Physics Eindhoven University of Technology, 5600MB Eindhoven, The Netherlands*

E-mail: crommun@upo.es; S.Calero@tue.nl

Abstract

In this work, we analyze the influence of small adsorbates on the vibrational spectra of Mg- and Zn-MOF-74 by means of first-principles calculations. In particular we consider the adsorption of four representative species of different interaction strengths: Ar, CO_2, H_2O and NH_3. Apart from a comprehensive characterization of the structural and energetic aspects of empty and loaded MOFs, we use a fully quantum *ab initio* approach to evaluate the Raman and IR activities of the normal modes, leading to the construction of the whole vibrational spectra. Under this approach, we are not only able to proceed with the complete assignment of the spectra in terms of the usual internal coordinates, but we can discern the most relevant vibrational fingerprints of the adsorbates and their impact on the whole MOF spectra. On the one hand, some of the typical vibrational modes of the small molecules are slightly shifted but still visible when adsorbed on the MOFs, especially those appearing at high wavenumbers where the empty MOFs lack of IR/Raman signals. On the other hand, some bands arising from the organic ligands are affected by the presence of the absorbates, displaying non-negligible frequency shifts, in agreement with recent experiments. We find a strong correlation between all these frequency shifts and the interaction strength of the adsorbate with the hosting framework. The findings presented in this work expand the capabilities of vibrational spectroscopy techniques to analyze porous materials and can be useful for the design of sensors and new devices based on MOF technology.

Keywords

Metal-organic framework, MOF-74, Vibrational spectroscopy, Density functional theory, Gas adsorption

Introduction

Metal-organic-frameworks (MOFs) are crystalline coordination polymers which combine metal centers with bridging organic linkers to constitute one- two- or three-dimensional porous structures with a high specific surface area. The shape and the size of the voids embedded in the MOFs structures are highly tunable from the experimental point of view, giving rise to a great variety of interesting applications like gas separation, CO_2 uptake, hydrogen storage or heterogeneous catalysis. All these applications are based on the high selectivity of the pore size with respect to some target adsorbates.[1] In particular, the metal centers of some MOFs have free coordination sites, which are called open metal sites or coordinatively unsaturated metal centers. These open metal sites usually act as strong binding sites, leading to an increased interaction with possible adsorbates, compared to other MOFs where the metal sites are fully coordinated.[2]

In this work we focus on the M-MOF-74 (M=Zn and Mg) system, also known as CPO-27, M_2(dobdc), M_2(dhtp), etc., first synthesized in 2005 by Yaghi's group.[3] It is an archetypal example of MOF constituted by single divalent metal ions (such as Fe, Co, Ni, Mn, Zn, Mg, etc.) pentacoordinated by oxygen atoms of 2,5-dioxo-1,4-benzenedicarboxylate ligands. Therefore, metal centers are really open sites because they have still a missing coordination site to achieve the ideal octahedral environment. In addition, MOF-74 possesses one-dimensional hexagonal porous channels with a pore size of about $10 - 12$ Å, following an hexagonal honeycomb structure and the free coordination site of the open metal centers is oriented inward to these channels. These features make MOF-74 a very appropriate candidate to most of the typical applications of MOFs and it has been widely studied in the recent literature.[4–9]

Despite all the recent progress, there are still many unanswered questions regarding the interaction between small adsorbates and the hosting frameworks. The adsorption of CO_2 is, by far, the most studied case of molecular adsorption on MOF-74, with many published works in the recent literature, both from the experimental and theoretical points of view.[10–15]

This is because MOF-74 is regarded as a promising porous material to perform CO_2 capture applications, as a consequence of its extraordinary uptake capacity combined with a facile regeneration[4,6,16] Nevertheless, the adsorption of strong polar molecules such as H_2O or NH_3 is not so well understood. These molecules strongly interact with the open metal sites of MOF-74 forming covalent bonds and are extremely difficult to track from the experimental point of view. In particular, water molecules may react with the open metal sites affecting the stability of MOF-74 crystal structure.[17,18]

In this work, we use a fully quantum *ab initio* approach to evaluate the IR/Raman activities[19,20] of the molecular vibrational modes in our system. First, we carry out a systematic assignment of the vibrational spectra of bare MOFs and then, we make a comprehensive study of the adsorption of four representative species of different interaction strengths: Ar, CO_2, H_2O and NH_3. We mainly focus on the study of IR and Raman spectra because vibrational spectroscopy is a widely used material characterization technique extremely sensitive to minor structural changes in the chemical bonding. Furthermore, it has proved to be a very appropriate technique to investigate the interaction between adsorbates and a host MOF,[17,18,21–25] since these interactions may induce changes in the dipole moments and dynamic polarizabilities of both entities. In fact, the extreme flexibility of some MOFs leads to remarkable structural deformations after gas adsorption.[26] In this way, the changes observed in the spectra of loaded MOFs with respect to the isolated adsorbates provide valuable information regarding possible structural changes upon adsorption. For example, the shortening of a bond in the adsorbate usually leads to blue frequency shifts in those modes associated to that bond. Conversely, a red shift of some active mode might reveal the weakening of the corresponding bond of the adsorbate molecule. However, this kind of analysis often gets complex because we have to take into account other factors that may have a remarkable influence on the vibrational spectra. For instance, the modification of the electric field by the electrostatic interaction between the host material and the adsorbates gives rise to a number of effects, such a strong variation in the IR/Raman activities of the modes, splitting be-

tween originally degenerate modes, alteration of the selection rules or unexpected frequency shifts. Moreover, it has been demonstrated that the frequency shifts experimented by small molecules adsorbed on zeolites strongly depend on the orientation of the adsorbed molecule with respect to the local electric field and also on the nature of the vibrational mode, finding opposite behaviors for flexion and stretching modes.[27] The small adsorbates considered in this work possess very few vibrational modes, which represents a clear advantage to track the possible changes in their active modes.

In this work, we study in detail the vibrational fingerprints of small adsorbates and their impact on the spectra of MOF-74. We find a remarkable correlation between the interaction strength between the adsorbate and the hosting MOF and the frequency shifts observed in the IR/Raman spectra of the loaded MOFs. Our results demonstrate that the typical vibrational modes of the small molecules suffer slight frequency shifts and other phenomena like band splittings when adsorbed on MOF-74. Moreover, some of these signals remain detectable in the high wavenumber region where the bare MOFs lack of vibrational signatures. Thus, vibrational spectroscopy could be a useful tool to detect and identify adsorbates leading to gas sensing applications. Additionally, those bands in the spectra associated to the organic linkers become also affected by the presence of the absorbates, displaying frequency shifts, in agreement with recent experiments.

Methods

Our analysis of the structural and vibrational properties in MOF-74 with various adsorbates is based on Density Functional Theory (DFT) calculations using the VASP (*Vienna Ab Initio Simulation Package*) code.[28] A plane-wave basis set with a kinetic energy cutoff of 425 eV was used to reproduce the total wavefunction of the studied systems. Pseudopotentials based on the projector augmented wave method[29,30] were used in combination with the Perdew-Burke-Ernzerhof (PBE) exchange and correlation functional.[31] The non-local van der Waals

interactions were taken into account using the semi-empirical D3 correction by S. Grimme.[32] This consideration is essential to obtain proper equilibrium geometries of the adsorbates and their corresponding adsorption energies. In this regard, previous assessment work in this topic[11,15,33] have shown that all the conventional van der Waals corrected functionals lead to reasonable and accurate results in this respect, without finding any preferential choice.

The isostructural M-MOF-74 series always presents the same hexagonal-rhomboedrical crystal symmetry represented by the centrosymmetric space group $R\overline{3}$ (no. 148). We restrict our analysis to M=Mg and Zn, which are non-magnetic closed shell ions. The conventional (hexagonal) unit cell of MOF-74 contains 162 atoms including 18 metal centers, while the primitive (rhombohedral) cell only 54 atoms (just one third). All the calculations in this paper are carried out in the primitive 54-atom cell with symmetry operations and periodic boundary conditions applied. The equilibrium geometries were obtained using a conjugate gradient algorithm in combination with electronic self-consistent loops, using a $2 \times 2 \times 2$ Monkhorst-Pack grid[34] to sample the reciprocal space. The stopping criterion for the structural optimization was that forces upon atoms had to be smaller than 0.005 eV/Å while each self-consistent electronic loop converged with a tolerance better than 10^{-6} eV. Such a strict criterion on forces was imposed to find a good energy minimum and ensure the reliability of the subsequent normal mode analysis. During the ionic relaxations all atomic positions were allowed to relax and no restrictions were considered either in the lattice vectors or in the cell volume. The minimal deviations from their initial configurations found after the geometrical optimization reveal that the original symmetry is preserved even in the presence of small adsorbates. The starting geometry was obtained from *in situ* X-ray and neutron diffraction experiments reported in the literature.[13,35] Since not all the adsorbates studied here were available from previous works, we slightly modified the input coordinates of related adsorbates. In any case all studied structures were fully resolved by the first-principles method described before.

Apart from the empty MOFs, we study the adsorption of four species of different nature:

Ar, CO_2, H_2O and NH_3. They present a wide range of interaction strengths that allow us to extract general conclusions about the impact of small adsorbates on the vibrational spectra. In all cases we consider one adsorbate per metal center. This equates to, a concentration of 8.24 mmol g^{-1} and 6.16 mmol g^{-1} for Mg-MOF-74 and Zn-MOF-74 respectively. The adsorption energies, sometimes referred as binding energies, are calculated by

$$\Delta E_{\text{ad}} = \frac{1}{n}(E[\text{MOF} + \text{mols}] - \text{E[MOF]} - \text{nE[mol]}), \tag{1}$$

where n is the number of adsorbed molecules (in our case n is always six), $E[\text{MOF} + \text{mols}]$ represents the energy of the loaded MOF with n adsorbed molecules and $E[\text{MOF}]$ and $E[\text{mol}]$ are the energies of the bare MOF and the isolated adsorbate respectively. The isolated molecules are calculated in large unit cells with sufficient distance between periodical images (>30 Å) to avoid any spurious interaction.

The vibrational properties of MOF-74 were investigated following a normal mode analysis under the harmonic approximation.[36,37] That is, the direct diagonalization of the mass-weighted Hessian matrix appearing in the eigenvalue problem of the equations of motions using normal coordinates. The Hessian matrix is numerically obtained through a finite differences algorithm which considers a total of six small displacements of ±0.02 Å per atom along the three Cartesian coordinates. Once the normal modes (eigenvectors and eigenfrequencies) are known the Raman and IR activities can be evaluated as described in detail in our previous work.[19,20] In brief, the Raman activity of the the nth normal mode is given by the variation of some elements (α_{ij}) of the polarizability tensor along that vibrational mode as[38]

$$I_n^{\text{Raman}} \propto \frac{1}{45}\left[45\left(\frac{d\alpha}{dQ_n}\right)_{eq}^2 + 7\left(\frac{d\beta}{dQ_n}\right)_{eq}^2\right], \tag{2}$$

where α and β are two invariants of the polarizability tensor given by:

$$\alpha = \frac{1}{3}(\alpha_{11} + \alpha_{22} + \alpha_{33}), \tag{3}$$

$$\beta^2 = \frac{1}{2}[(\alpha_{11} - \alpha_{22})^2 + (\alpha_{11} - \alpha_{33})^2 + (\alpha_{22} - \alpha_{33})^2 + 6(\alpha_{12}^2 + \alpha_{13}^2 + \alpha_{23}^2)]. \tag{4}$$

Here the derivatives of Eq. (2) are numerically evaluated using two geometries slightly displaced along the corresponding normal mode with respect to the equilibrium position.

The IR intensity of a normal mode is related to the square of the variation of the electric dipole moment along the vibration.[36] This result can be expressed also in terms of the Born effective charges $Z^*_{\alpha\beta,\tau}$ as[39]

$$I_n^{\mathrm{IR}} \propto \sum_{\alpha=1}^{3} \left| \sum_{\beta=1}^{3} \sum_{\tau=1}^{N} Z^*_{\alpha\beta,\tau} A^{\tau}_{\beta,n} \right|^2, \tag{5}$$

where N is the number of atoms and $A^{\tau}_{\beta,n}$ is the nth eigenvector. Notice that both the Born effective charges and the polarizability tensor, together with other relevant electronic properties, can be calculated within DFT methods in the frame of the linear response theory using Density Functional Perturbation Theory (DFPT).[40,41] Finally, once the intensity of all modes has been calculated, a discrete collection of intensities associated with each normal mode is obtained and the complete spectrum can be constructed as a sum of continuous Lorentzian functions centered in each eigenfrequency. A broadening of $\gamma = 3$ cm^{-1} is enough to keep a good resolution while providing the look and feel of experimental spectra.

Crystal structure

The crystal structure of MOF-74 consists of an arrangement of symmetrically-distributed parallel channels with hexagonal section, as depicted in Fig. 1. The metal centers distributed along the chains display a free coordination site pointing inwards, which is accessible to bind small molecules like CO_2, NH_3, H_2O or light hydrocarbons, reaching an octahedral envi-

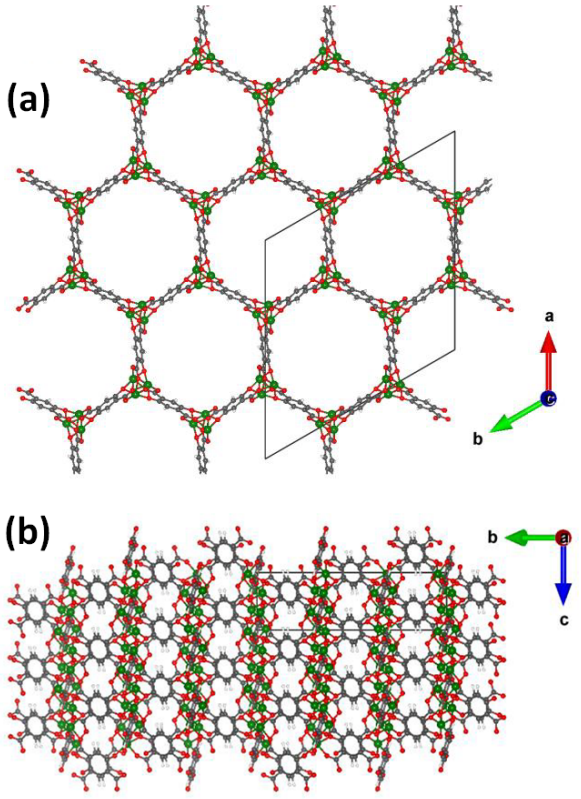

Figure 1: Top and side views of the MOF-74 crystal structure. (a) Along the c-axis displaying the parallel hexagonal channels and (b) along the a-axis where the metal center (green balls) chains are shown. Notice that the unit cell is highlighted in each case.

ronment for the metal ions. The crystal structure belongs to the hexagonal-rhomboedrical system (space group $R\bar{3}$) whose conventional unit cell has 162 total atoms while the primitive cell only contains 54 atoms, including six metal centers. Thus, this system is especially appropriate to be explored by means of quantum first-principles calculations.

As shown in Table 1 (and Tables S1 and S2 in the Supporting Information), the agreement between our calculated structural parameters and previous calculations and experimental data is remarkable. First, we analyze the structures of the empty MOFs, which have been already studied in depth by first principles calculations [15,42–45] and several experimental techniques like X-ray and neutron diffraction. [10,13,15,46,47] Our calculations yield very similar values of lattice parameters compared to those experimentally reported. We get a minimal overestimation in the basal plane and a minor underestimation of the cell height, especially

Table 1: Structural parameters of the unit cells. The lattice constants in the conventional hexagonal cell (a and c), the M–O distances including the average of the four planar ligands ($\langle$M–O$\rangle_{\rm pl}$) and the apical one (M–$O_{\rm ap}$), together with the distance between the adsorbate and the open metal site (M–A). We compare our results with experimental ones whenever possible.

Metal	Adsorbate	a (Å)	c (Å)	$\langle$M–O$\rangle_{\rm pl}$ (Å)	M–$O_{\rm ap}$ (Å)	M–A (Å)	ref.
Mg	Empty	25.962	6.807	2.02	2.06	**	This work
	Empty	25.921	6.8625	2.06	2.17	**	47
	Ar	25.844	6.779	2.015	2.06	3.22	This work
	CO_2	25.762	6.749	2.02	2.06	2.33	This work
	CO_2	25.824	6.8904	-	-	2.28-2.30	47
	H_2O	25.689	6.823	2.04	2.09	2.18	This work
	NH_3	25.717	6.843	2.05	2.09	2.22	This work
Zn	Empty	25.874	6.616	2.03	2.23	**	This work
	Empty	25.89	6.82	2.05	2.08	**	15
	Ar	25.724	6.581	2.03	2.23	3.47	This work
	CO_2	25.548	6.549	2.03	2.28	2.82	This work
	H_2O	25.862	6.331	2.04	**	2.24	This work
	NH_3	25.777	6.798	2.09	2.20	2.16	This work

in the case of Zn (around a 3%). Despite being isostructural the volume cell of Zn-MOF-74 is slightly smaller than the one of Mg-MOF-74, a trend which is successfully reproduced in our calculations. Our results are also in agreement with previous calculations using similar methodologies[15,42–45] (see Tables S1 and S2 in the Supporting Information). Minor variations can be found due to subtle differences in some secondary input parameters, that can be checked in the cited references.

Adsorption of small molecules

In this study we consider the presence of a total of four adsorbates, which cover a broad range of interaction strength. In particular, we study the adsorption of a noble gas (Ar), a non-polar molecule (CO_2) and two strongly polar and hydrogen-bond forming molecules (H_2O and NH_3). All of them adsorb on the open metal sites of MOF-74 in order to achieve the typical octahedral environment of the metal ion, as shown in the structures of Fig. 2 (check all the bond lengths in Table 1). The original coordination sphere of metal centers is consists

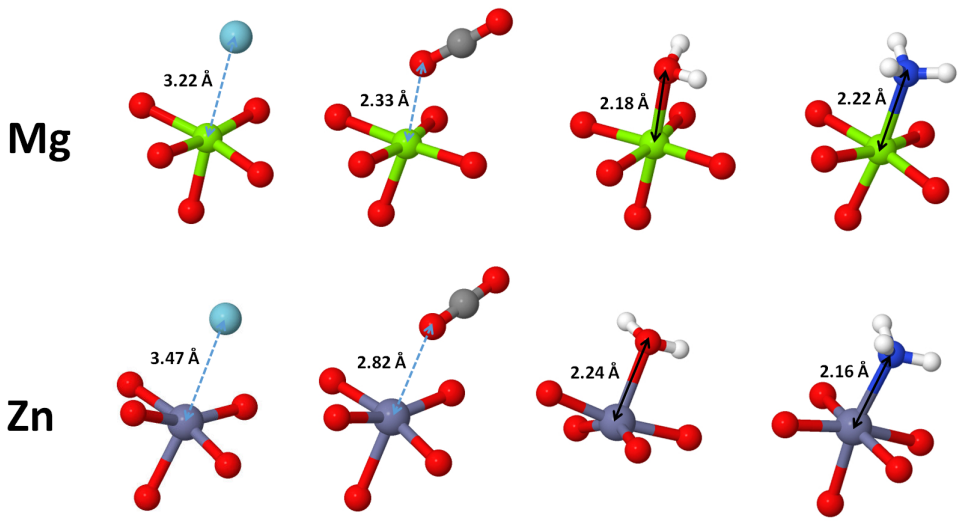

Figure 2: Detailed structures of the open metal sites (Zn and Mg) coordinated with the adsorbed molecules. From left to right: Ar, CO_2, H_2O and NH_3.

of five O atoms belonging to carboxylate and phenolate groups of four organic linkers. Two phenolate groups and two carboxylate groups form the square base of the octahedron while a fifth carboxylate group acts as apical and finally one adsorbate may complete the octahedral coordination. There is a single exception that is the water adsorbed on Zn-MOF-74 where the former apical carboxylate O-ligand is removed from the first coordination sphere and a highly distorted pentacoordinated structure emerges. This can be viewed as a slightly distorted seesaw geometry (with four O-ligands) with a fifth coordination site pointing to the MOF-74 channel. All other structures display the usual octahedral geometry close to the ideal parameters in the case of Mg and with small distortions in the case of Zn. Strongly polar adsorbates like H_2O and NH_3 induce the most noticeable changes in the whole structure of the MOF, as deduced from the values of the lattice parameters collected in Table 1. That is a considerable shortening along the *c*-axis especially in the case of water on Zn-MOF-74, in agreement with previous calculations.[44] This is one of the first signs of instability produced by the presence of water, which is not affecting so much the structure of Mg-MOF-74, revealing a higher stability against water. Conversely, the impact of weakly interacting species like Ar or CO_2 on the whole structure is not significant as we will discuss later.

Table 1 together with Table S2 in the Supporting Information, collect some relevant structural parameters related to the coordination complexes formed in MOF-74 after adsorption. As expected, the presence of neutral Ar atoms in the channels of MOF-74 barely affects the structure, displaying a very limited influence. This is a consequence of the weak adsorption revealed by large adsorption distances of 3.22 Å and 3.47 Å, typical of adsorbates interacting solely through weak dispersion forces. CO_2 adsorption on MOF-74 displays a similar behavior. The crystal symmetry is preserved after adsorption but a small shrinkage of the unit cell with increasing CO_2 concentration has been reported in Mg-MOF-74[47] by neutron diffraction experiments. This trend was later confirmed for other metals[13] following a similar experimental approach. The CO_2 molecule physisorbs on the open metal sites of MOF-74 through one of the O atoms, leading to moderate adsorption distances of 2.33 Å and 2.82 Å for Mg-MOF-74 and Zn-MOF-74 respectively. These values are in agreement with previous calculations and also supported by experimental measurements that suggest a strong physisorption of the CO_2 molecules, more intense than a purely van der Waals adsorption. This is a consequence of the interaction between the quadrupole moment of the molecules and the electric field of the metal ions.[10] The adsorption angle ∠M–O–C is also a relevant structural parameter that deserves some attention. Neutron diffraction experiments[13,47] point out values of 131° and 117° for Mg-MOF-74 and Zn-MOF-74 respectively, in close agreement with our calculations (132.1° and 115.5°). In addition the CO_2 molecules remain linear after adsorption with angles around 178°. Notice that, although previous neutron diffraction experiments[13,47] have revealed other secondary adsorption sites for higher concentrations, here, we focus exclusively on the adsorption directly on the open metal site. This is because all the vibrational signatures arising from less strongly bonded or freely flowing molecules will have a much lower impact on the IR/Raman spectra.

Conversely highly polar molecules like water or ammonia display much closer adsorption distances similarly to the other O-ligands of the framework. In particular H_2O molecules bind through the O atom displaying bond lengths of 2.18 Å and 2.24 Å for Mg-MOF-74 and

Zn-MOF-74 respectively. These values are also compatible with experimental observations in hydrated MOF-74 with other metals, which reveal also short bond distances of 2.08 Å (Ni-MOF-74)[48] and 2.16 Å (Co-MOF-74).[49] Finally, NH_3 molecules present similar adsorption distances of 2.22 Å in Mg-MOF-74 and 2.16 Å in Zn-MOF-74.

We have calculated the adsorption energies of the four adsorbates considered in this work following a twofold purpose. On the one hand, these values serve as a benchmark that confirms the reliability of our methodology, especially in the case of CO_2 where a great amount of previous calculations and experimental measurements are available in the literature. Besides, the obtained values of adsorption energies provide useful information about the strength of the interactions between the different adsorbates and the open metal sites in MOF-74.

In Table 2 we collect the adsorption energies calculated on Mg-MOF-74 and Zn-MOF-74. We begin analyzing the adsorption of CO_2 molecules because there is a number of previous

Table 2: Calculated adsorption energies (ΔE_{ad}) of the four adsorbates considered in this work. In the case of CO_2 we compare our results with previous calculations and experimental values reported in the literature. Those methods labeled with an asterisk denote that they are calculating single-molecule adsorption.

	ΔE_{ad} (kJ/mol)			
	Mg	Zn	Method	ref.
Ar	−11.3	−11.1	PBE+D3	This work
CO_2	−39.8	−32.3	PBE+D3	This work
CO_2	−43.5	−26.8	exp.	13
CO_2	−39.7	−31.8	PBE+D3*	15
CO_2	−43.6	−32.1	rev-vdW-DF2*	15
CO_2	−42.31	−30.53	PBE-D2	43
CO_2	−41.4	−34.0	PBE-D2	50
CO_2	−41.5	−35.2	B3LYP+D	42
CO_2	−42.4	–	PBE-D2	11
CO_2	−43.4	–	PBE-D2	33
H_2O	−76.5	−59.8	PBE+D3	This work
H_2O	−73.33	–	vdW-DF	51
H_2O	−81.3	−62.5	PBE+D3*	15
H_2O	−81.2	−60.5	rev-vdW-DF2*	15
NH_3	−92.6	−83.5	PBE+D3	This work

results to compare with.[11,13,15,33,42,43,50,52] As we can see, the adsorption energies obtained for CO_2 are in very good agreement with previous results using similar methodologies, revealing a stronger interaction with Mg sites compared to Zn atoms. This trend has been experimentally confirmed by W. L. Queen, *et al.*[13] There are other studies reporting basically the same values of experimental adsorption energies of CO_2 on Mg-MOF-74,[4,6] while others point out to slightly larger values.[16,53]

Regarding other adsorbates, the amount of previous results is scarce. First-principles calculations have predicted low adsorption energy values ($\sim$ 10 kJ/mol) for Xe and Kr on MOF-74,[54] which is consistent with our values obtained for Ar adsorption. Very similar values of isosteric heat of adsorption has been measured for H_2 on Mg-MOF-74 (-10.1 kJ/mol) and Zn-MOF-74 (-10.1 kJ/mol)[46] and other metals.[23,46] The case of strongly interacting adosrbates like water or ammonia is extremely challenging from the experimental point of view, because water molecules react with the coordinatively unsaturated metal sites leading to complex chemical scenarios.[17,18] This is the reason for the total absence of reliable adsorption heat measurements for these adsorbates and only very few calculations are available for water adsorption,[15,51] which are however, in agreement with our own estimations. It is worth mentioning that, except in the case of Ar where the adsorption energies are almost identical, Mg-MOF-74 displays systematically higher adsorption energies, revealing a greater reactivity.

Vibrational Spectra of empty MOFs

With the approach described in the Methods section we have calculated the Raman and IR spectra of bare Mg-MOF-74 and Zn-MOF-74, which are shown in Fig. 3. Our normal mode analysis allows us to perform a complete assignment of the vibrational spectra revealing the nature of the molecular vibrations in terms of the usual internal coordinates. We can distinguish two distinctive regions in the vibrational spectra. On the one hand, we find a

low wavenumber region (<700 cm^{-1}) where the active bands mainly involve the vibrations affecting the metal centers. Due to the noticeable mass difference between Mg and Zn, the observed features are clearly distinguishable, with remarkable shifts in the positions of the active bands. In contrast, above 700 cm^{-1}, all spectra are rather similar, since most of the active modes in that region belong to the organic ligands in the structure.

The low wavenumber region is characterized by vibrational modes involving the metal centers accompanied by low energy collective vibrations and lattice modes. The IR spectrum of Mg-MOF-74 displays a strong band at 394 cm^{-1} surrounded by two weaker signals at 371 y 426 cm^{-1}. The IR spectrum Zn-MOF-74, however, presents noticeable bands at 212, 257 and 292 cm^{-1}, although their intensities are much lower than the corresponding bands in Mg-

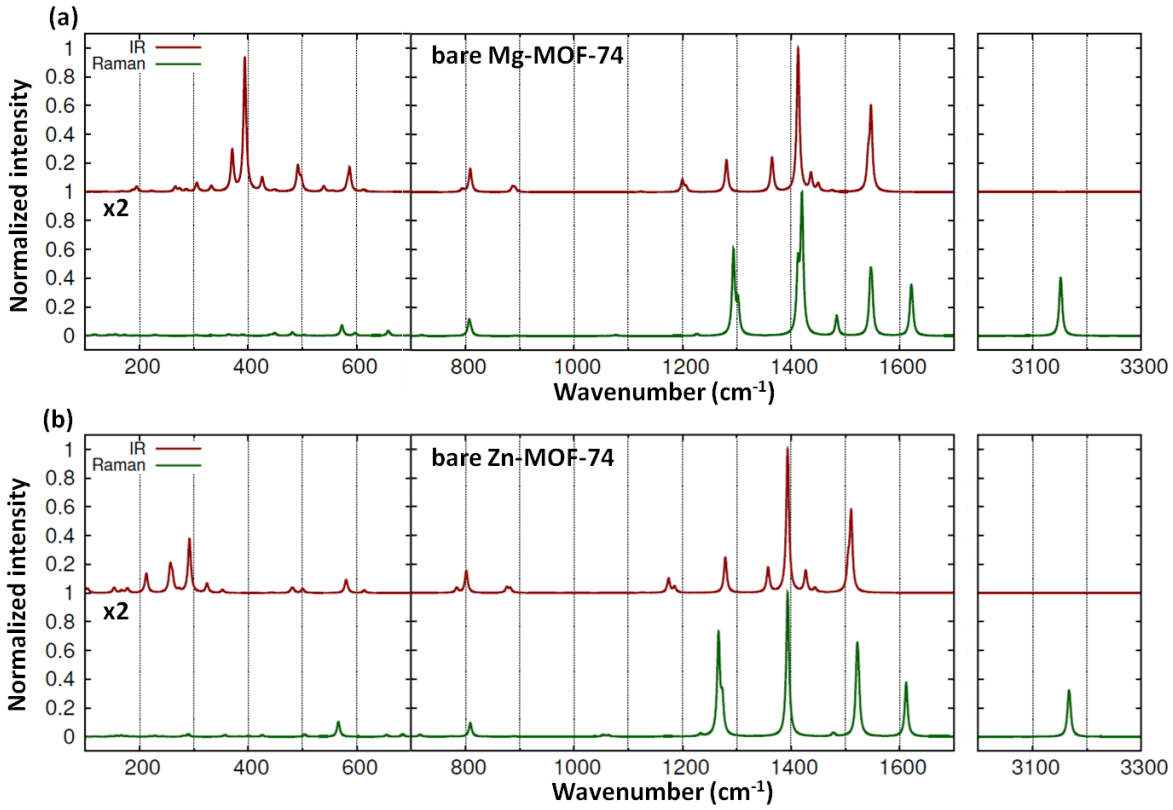

Figure 3: Calculated Raman and IR spectra for bare Mg-MOF-74 (a) and bare Zn-MOF-74 (b). The intensities are normalized to one with respect to the strongest band but the low wavenumber regions (<700 cm^{-1}) have been multiplied by a factor 2 only to make features more apparent.

MOF-74 at $\sim$ 426 cm^{-1}, as shown on the left side of Fig. 3. The Raman spectra show very limited activity in this range. Although some weak signals can be detected (449 and 481 cm^{-1} for Mg-MOF-74 and 290 cm^{-1} for Zn-MOF-74), this activity cannot be entirely ascribed to the metal center modes but to more complex lattice vibrations. The visual inspection of the modes responsible for these bands reveals that the Mg vibrations show larger amplitudes than those involving Zn^{2+} ions. The molecular vibrations are not completely equivalent between Mg and Zn. While some vibrations of Mg-MOF-74 resemble Mg–O stretching modes, we are unable to assign similar modes for Zn-MOF-74. In any case, it is complicated to describe these metal modes in terms of classical vibrations due to their pentacoordinated environment. In this way, a possible Mg–O or Zn–O stretching vibration implies further movements in other O atoms of the first coordination sphere, giving rise to wagging or bending O–Mg–O or O–Zn–O modes or even more complex modes. In spite of all these difficulties, there are still a limited number of vibrational modes that could be considered as equivalent between Mg and Zn MOFs. They are located at 587/580 cm^{-1} 498/480 cm^{-1} 394/353 cm^{-1} and 332/290 cm^{-1} for Mg- and Zn-MOF-74 respectively.

It is worth noting that such differences between spectra cannot be exclusively attributed to the distinctive atomic weights of Mg and Zn ions. This mass difference could account for substantial frequency shifts but it cannot explain the qualitative discrepancies found. More likely, these differences are related to the very different electronic configurations of the two metal centers. Although Mg and Zn ions are closed shell systems, Mg ions lack of d orbitals while Zn ions possess fully occupied $3d$ orbitals. Although these metal-organic modes are rarely considered in the literature, a recently released book by Maslowsky[55] (and references therein) collects some useful examples of related organometallic compounds that enables a valuable comparison. In a Mg adduct obtained through the reaction of tris(8-hydroxyquinolinate)aluminium and Mg vapor IR experiments suggest signals at 420 and 614 cm^{-1} for Mg–C and Mg–O stretching modes. A comprehensive IR and Raman study of various polycrystalline complexes of Grignard reagents (namely, methyl and ethyl magnesium

bromides complexes like $RMgBr{\cdot}2O(C_2H_5)_2$ and some of their deuterated derivatives) assigns Mg–O stretching modes at 301 and 317 cm^{-1}. All these assignments are in agreement with our results. In the case of Zn vibrational modes, we can compare with a number of bidentate carboxylate complexes that present a rather similar coordination environment. Mononuclear zinc acetates display a tetrahedral geometry which leads to active Raman bands at 229 and 264 cm^{-1}, as a consequence of Zn–O stretching modes in the tetrahedrons.[56] Additionally, related oxo-tetranuclear complexes display a noticeable IR signal at relatively higher wavenumber (i.e. 336 cm^{-1}) and also in Raman (342 cm^{-1}) also due to Zn–O stretch, whereas vibrations involving Zn–Zn bonds are visible at 225 cm^{-1} in the Raman spectrum.[57]

For higher wavenumbers, we find the characteristic bands associated to typical vibrational modes of organic molecules. In the particular case of MOF-74, those arising from the phenolate and carboxylate groups and the benzene rings of the ligands. In Table 3, we have collected the most representative bands of the spectra, including a brief description of their

Table 3: Systematic assignment of the most relevant IR and Raman bands (in cm^{-1}) of bare Mg-MOF-74 and Zn-MOF-74. Notice that the mode descriptions is made in terms of the usual internal coordinates, where a and s denote asymmetric and symmetric respectively, C_c is the C atom of the carboxylate group, bz the benzene ring and ph phenolate.

Mg-MOF-74		Zn-MOF-74		
IR	Raman	IR	Raman	Description
	3151		3167	CH stretching
	1622		1612	CC (bz) stretching
	1547		1522	(a) COO^- stretching
1541		1511		(a) COO^- stretching
	1484		1478	CC (bz) and COO^- stretching
1450		1444		CC (bz), CC_c and CO^- (ph) stretching and CH bending
1437		1427		CC (bz) and CC_c stretching and CH bending
1420	1413	1394	1394	CC_c stretching and in-plane ring deformation
1365		1358		CC (bz), CC_c and CO^- (ph) stretching
	1294		1267	CC (bz) and (s) CO^- (ph) stretching
1281		1279		(a) CC (bz) stretching
1206		1185		CH and ring bending
890		882		CH, ring and COO^- bending and CC_c stretching
809		801		ring breathing and (s) COO^- bending
	807		809	ring breathing and COO^- bending

active modes. The first noticeable bands in this region appear at ∼800 cm^{-1} as a consequence of breathing and soft bending modes in the benzene rings together with extra bending modes of the carboxylate groups. For higher wavenumber ($1200 - 1450$ cm^{-1}), the predominant modes become the stretching modes located on C–C bonds of the benzene rings, C–C_c bonds and C–O^- phenolate bonds. Above 1400 cm^{-1} the active modes are mainly dominated by stretching modes of the carboxylate groups, although there is an important contribution of C–C stretching modes of the benzene rings, giving rise to a Raman band at 1620 cm^{-1} in Mg-MOF-74 and at 1612 cm^{-1} in Zn-MOF-74. Finally, the high wavenumber region (>1700 cm^{-1} lacks of any relevant IR/Raman signature except for a single peak at ~ 3150 cm^{-1} in the Raman spectra, arising from C–H stretching modes in benzene rings. As expected, the most intense band of the spectra arise from the COO^- and C–O^- stretching modes of carboxylate and phenolate groups. This general assignment is in good agreement with previous experimental work.[17]

According to Table 3, we find exactly the same vibrational fingerprints in both MOFs with Zn and Mg. However, notice that the Zn-MOF-74 bands are slightly shifted to lower wavenumbers (overall $10 - 20$ cm^{-1}) compared to those of Mg-MOF-74. This feature is also in agreement with the observed trends in the experimental spectra.[17] It is worth noting that our calculations for MOF-74 fulfill the rule of mutual exclusion in molecular spectroscopy, as expected for a centrosymmetric system. This principle states that no normal mode can be simultaneously active in IR and Raman spectroscopy if the system possesses an inversion center,[58] such as in the case of the $R\bar{3}$ crystal space group of MOF-74. However, there is a single exception for one active band (located at 1413 cm^{-1} in Mg-MOF-74 and 1393 cm^{-1} in Zn-MOF-74), which is IR and Raman active simultaneously. This is a straightforward consequence of the geometrical optimization performed where volume cell changes were allowed, and therefore slight deviation from the original rhombohedral symmetry may occur.

The impact of small adsorbates on the vibrational spectra

As we have pointed out, vibrational spectroscopy provides valuable information about the molecular structure of the analyzed samples. Therefore, it constitutes a very appropriate technique to probe the interaction between small molecules and the hosting MOF. Now, we study in detail the changes produced in the IR/Raman spectra of CO_2, H_2O and NH_3 once adsorbed on MOF-74. In all cases we will consider a fixed load of one adsorbate per metal center since variations in the adsorbate concentration do not affect the positions of the bands but mainly the relative IR/Raman intensities,[21,22] which we are not going to discuss in depth. For NH_3 and H_2O adsorption it is also possible to find some fingerprints associated to the formation of intermolecular H-bonds.[17,24]

The CO_2 molecule possesses a linear geometry with a high quadrupole moment and polarizability, which presents four vibrational normal modes: a C=O asymmetric (υ_3), and a symmetric stretching (υ_1) and a doubly degenerated bending mode (υ_2). Notice that, in the following, we have used the nomenclature established by Herzberg[59] to denote the vibrational normal modes. The CO_2 υ_1 stretching mode is the only Raman active mode while all the rest are IR active attending to the mutual exclusion principle of vibrational spectroscopy. (see Fig. S3 in the Supporting Information). Our calculations predict the emergence of forbidden bands, the lack of degeneration of υ_2, the splitting of the band associated to the υ_3 mode, and frequency shifts.

In Table S3 of the Supporting Information, we have collected the IR/Raman signals corresponding to the vibrational modes associated to the adsorbed CO_2 molecules and compare with the gas phase vibrational bands. According to Table S3, all associated modes become active in IR and Raman spectra, although those previously forbidden present a low IR/Raman activity. Namely, the υ_1 mode becomes IR active while υ_2 and υ_3 become Raman active because the rule of mutual exclusion is not valid anymore after adsorption. This is a common feature of adsorbed molecules as a consequence of the absence of an inversion center in the adsorbed configuration. For instance, the IR inactive stretching mode of the

H_2 molecule becomes active when adsorbed on MOF-74 with several metals.[60]

The double-degenerated υ_2 bending mode of gas phase CO_2 is not fully degenerate in our calculations due to some numerical uncertainty. However, when adsorbed on the open metal sites of MOF-74 they become completely non-degenerate bands. For instance, in the IR spectra of the loaded MOFs we get a splitting of 12 cm^{-1} in Mg-MOF and 8 cm^{-1} in Zn-MOF. The same effect is also observed in the Raman spectra. This effect is consistent with the sloped adsorption configuration discussed for the CO_2 molecules. The lack of degeneration in the υ_2 bending mode is a more general phenomenon, experimentally observed in other MOFs. For instance, in Cr-MIL-53 a similar splitting of ~ 10 cm^{-1} is found in the IR spectrum.[61] Therefore, this splitting is a direct consequence of the reduction of the symmetry of the molecule once it is adsorbed on the open metal sites. A similar effect is found also in the υ_3 asymmetric stretching mode, where a noticeable splitting is observed after adsorption. Two separated signals at 2349 and 2361 cm^{-1} appear in the IR spectrum of Zn-MOF-74 while a similar splitting between 2369 and 2374 cm^{-1} is found in the Raman spectrum of Mg-MOF-74.

We can notice also that CO_2 bands suffer different frequency shifts when adsorbed on MOF-74. In particular, experiments reveal a systematic shift to lower wavenumbers of all CO_2 modes with respect to the gas phase reference, except for the case of υ_3 mode in Mg-MOF-74, where a slight increment of $3-4$ cm^{-1} is observed.[21,53] Our calculations successfully reproduce these trends, including the blue shift of the asymmetric υ_3 mode which goes from 2363 cm^{-1} in gas phase CO_2 to 2368 cm^{-1} or $2369-2374$ cm^{-1} in the IR and Raman spectra respectively. The reason for this distinctive behavior in Mg-MOF-74 seems to be related to the absence of d orbitals in the Mg ions, which ultimately prevents a π backbonding mechanism found in the MOF-74 containing transition metals.[21,62] Moreover, further studies[24] have demonstrated that the blue shift of υ_3 is exclusively found in Mg-MOF-74 and not observed in others metals, such as Zn, Ni, Co or Mn, giving extra support to the relevance of metal d orbitals in the backbonding.

The water molecules have three non-degenerate normal modes which are all active in Raman and IR due to the absence of a symmetry center. After adsorption on MOF-74, our theoretical calculations predict that all of them are subjected to red shifts with respect to the gas phase molecule (see Table S4 in the Supporting Information). These frequency shifts are in some cases as large as 100 cm^{-1}, much more pronounced in comparison with CO_2 shifts. This fact reveals that H_2O molecules are strongly chemisorbed to the open metal sites, likely, forming a dative bond. However, the magnitude of these frequency shifts are not large enough to justify the presence of H-bonds between water molecules and carboxylate or phenolate groups in MOF-74. Our calculations are in overall agreement with previously reported experiments carried out at low pressure.[17] The trends in frequency shifts also coincide with those experimentally reported. That is, stretching modes (υ_1 and υ_3) suffer strong frequency shifts of $80 - 100$ cm^{-1} while υ_2, a bending mode essentially remains unaltered (4 cm^{-1} red shifted in the calculations vs. 15 cm^{-1} blue shifted in the experiments).

The ammonia molecule is slightly more complex, compared to CO_2 and H_2O, with a total of six vibrational modes, with two pairs of double-degenerated modes. Essentially, the effects on ammonia modes after adsorption on MOF-74 are very similar to the ones already described for CO_2 and H_2O adsorption, as deduced from Table S5 in the Supporting Information. On the one hand, we appreciate moderate frequency shifts (both blue and red), in agreement with experimental results.[24] These shifts are more evident in the case of Zn-MOF-74. On the other hand, we observe a full breakdown of the double-degenerated modes, similarly to the CO_2 case, but with higher splittings. These vibrational fingerprints reveal a scenario rather similar to the one described for water, that is, a strong chemisorption of the NH_3 molecules without the presence of H-bonds. This behavior in frequency shifts is a trustworthy proof to confirm a strong chemisorption. For instance, a very similar behavior is observed in the vibrational spectra of ammonia loaded Cu-HKUST-1,[63] which also possesses open metal sites. Conversely, in other MOFs, like MOF-7 or MOF-177, without open metal sites, the ammonia signal remain mainly unaltered after adsorption.[64]

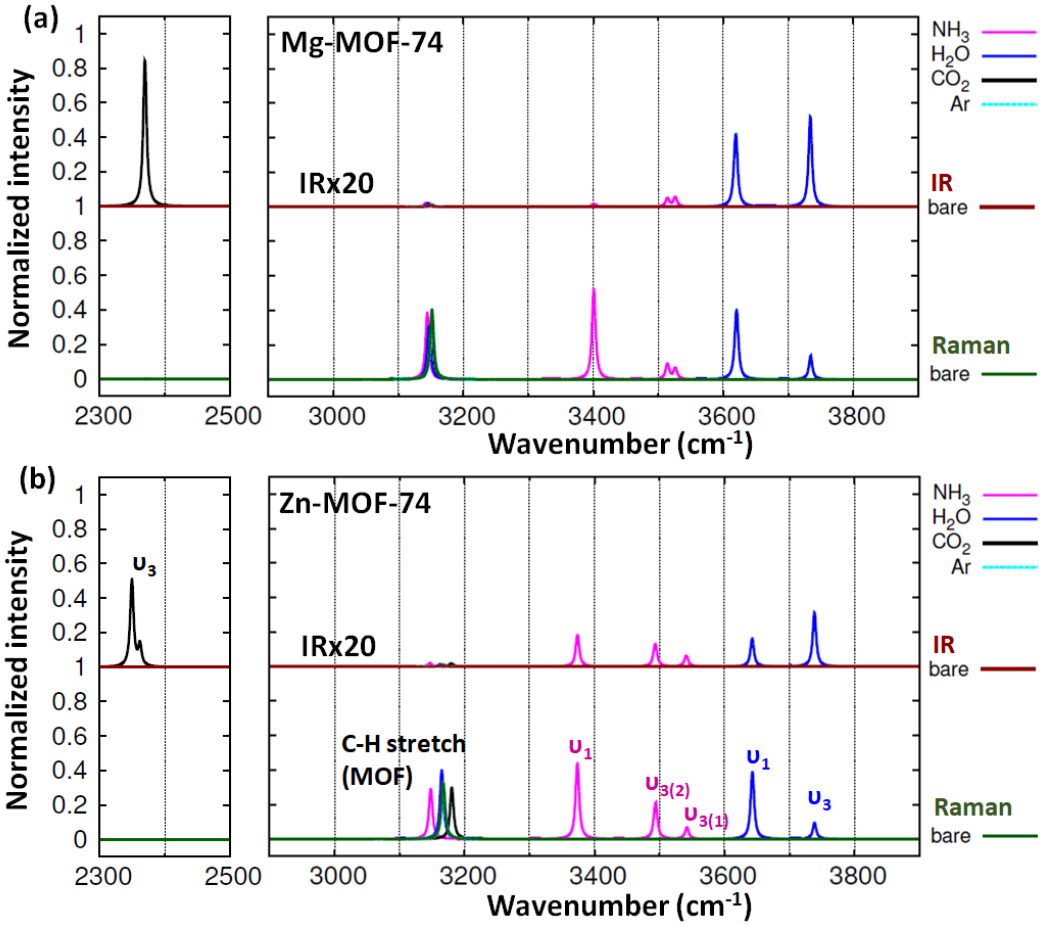

Figure 4: High wavenumber region of the calculated IR and Raman espectra of Mg-MOF-74 (a) and Mg-MOF-74 (b) upon adsorption of Ar, CO_2, H_2O and NH_3. In this region of the spectra, most of the IR/Raman signals arise from the molecular vibrations of the adsorbed molecules. The intensities in the spectra are normalized to one with respect to the strongest band but the IR signals above 2900 cm^{-1} have been multiplied by a factor of 20 only to make features more apparent.

It is worth noting that a good number of interesting adosrbates, including the ones considered in this work, display active modes in the high wavenumber region of the vibrational spectra. This fact may represent a very useful aspect from the experimental point of view, since many standard MOFs lack of vibrational modes in that wavenumber region. To illustrate this feature, in Fig 4 we show the high energy region of the vibrational spectra of loaded MOFs, where we can easily distinguish every band associated with each molecule, as we highlight in the Zn-MOF-74 spectra (lower panel of Fig 4). In this regard, a detailed knowledge of the positions of these bands can be useful to detect the presence of a given

adsorbed molecule on the open metal sites, with potential application in gas sensing or to design new devices aimed to detect a specific guest molecule.

Up to now, we have focused on the evolution of the adsorbate signals embedded in vibrational spectra of loaded MOFs. However, it is also of interest to study the possible changes in the vibrational bands associated to the organic linkers induced by the presence of the four adosrbates considered in this work. See the whole vibrational spectra of loaded MOFs in Figs. S1 and S2 in the Supporting Information. The thorough analysis of the bare MOFs carried out in the previous section establishes a good basis to start this analysis. Thus, we focus on the region between 1100 cm^{-1} and 1700 cm^{-1} where the strongest bands of the spectra appear. We can appreciate that the positions of organic bands of the spectra are shifted with respect to the ones in bare MOFs when hosting adsorbates as shown in Fig. 5.

First of all, we can distinguish two behaviors, one for weakly bonded adsorbates (Ar and CO_2) and another for the strongly chemisorbed molecules (H_2O and NH_3). In the first case we observe small energy shifts, always displaced to lower energies, except for a couple of exceptions for CO_2 adsorbed on Mg-MOF-74. As expected, the vibrational spectra of Ar adsorbed MOFs resemble very much to those of bare MOFs with frequency shifts smaller than those for CO_2. On the contrary, band shifts for H_2O and NH_3 are larger in magnitude but they are either blue or red shifted, approximately half and half. This behavior is very similar for Mg-MOF-74 and Zn-MOF-74, displaying equivalent displacements band by band.

Previous experiments carried out in Co-MOF-74[65] suggest that these frequency shifts experimented in the Raman spectra after adsorption of several adsorbates could be a fingerprint of each molecule. To get a more quantitative insight in this regard, we have collected in Tables S6-S9 in the Supporting Information all the frequency shifts observed for the most representative bands in Mg-MOF-74 and Zn-MOF-74 spectra for the four adsorbates considered in this work. If we assume as a natural ordering the adsorbate series by decreasing adsorption energy, that is NH_3>H_2O>CO_2>Ar, we can find a few bands of the spectra that follow exactly this trend. For instance, in the case of Mg-MOF-74, the following bands

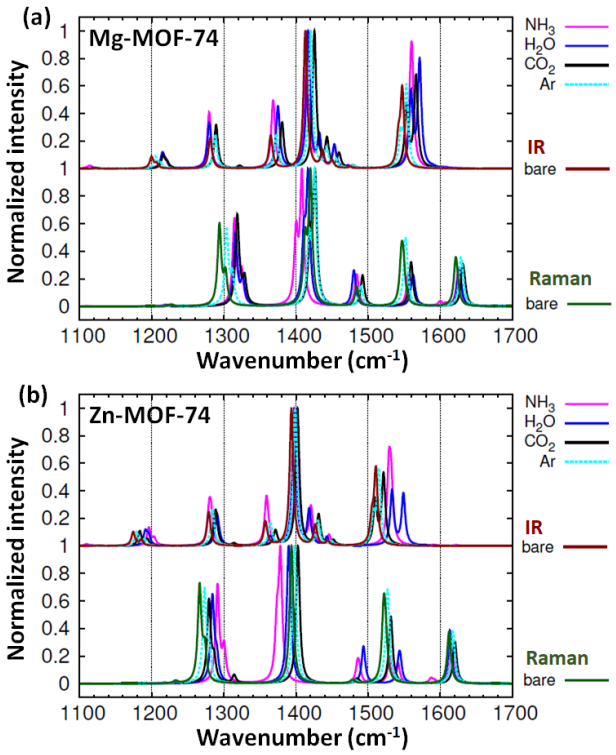

Figure 5: Mid wavenumber region of the calculated IR and Raman spectra of Mg-MOF-74 (a) and Mg-MOF-74 (b) upon adsorption of Ar, CO_2, H_2O and NH_3. Notice the frequency shift obtained in the most of the vibrational bands of the spectra after adsorption.

of the Raman spectra show this reasonable trend: at 3151 cm^{-1} (shifts in cm^{-1} for the cited series: $-7, -4, -1, 7$ and assignment; CH stretching), 1420 cm^{-1} ($-13, -3.5, 6, 7$, CC_C stretching), 1226 cm^{-1} ($-8.5, -7, -3.5, 1$, CH and benzene ring in-plane bending), or 807 cm^{-1} ($-11, -3, 1, 1$, ring breathing). Similarly, for Zn-MOF-74 we find also a few examples compatible with this tendency in frequency shifts. They are in the IR spectra at 1185 cm^{-1} ($17.5, 9.5, 8.5, 4.5$, CH and benzene ring in-plane bending) and 1174 cm^{-1} ($22, 17.5, 8.5, 4.5$, CH and benzene ring in-plane bending). Although these results reveal a strong correlation between adsorbate-MOF interaction and frequency shift, it is difficult to extract further quantitative trends considering only four adsorbates. This is because changes in the spectra after adsorption are due to either spatial changes in the adsorption configurations of molecules or electronic rearrangements along the vibrational mode. In the first case, often, the modification (shortening/stretching) of some bond lengths is found, leading to frequency

shifts correlated with the adsorption strength. Conversely, in those vibrations in which only electronic charge rearrangements are found, it will be very hard to find any remarkable frequency shift tendency, but only minor changes difficult to rationalize. Furthermore, in some cases a non-trivial interplay between the geometric and electronic contributions may be found, making, this distinction difficult to discern. These issues could be overcome by considering a much larger number of adsorbates. Unfortunately, this is unaffordable from the computational point of view at present, but we leave it for future work to expand this study, in the search of possible scaling laws or universal relations for different adsorbarte series.

Conclusions

In summary, we have studied the adsorption of four species on the open metal sites of MOF-74, namely Ar, CO_2, H_2O and NH_3 by quantum first-principles calculations. The selected adsorbate series covers a broad range of adsorption energies, ranging from weakly bonded physisorbed states to strong covalent attachment. In all cases, we find a good agreement between our results regarding adsorption energies and crystal structure and available experimental measurements. In a second step, we focus on the vibrational spectra of bare MOF-74 and their changes upon adsorption. We pay special attention to the description of the vibrational modes involving the metal centers, which appear at low energy and are rarely considered in the specialized literature. We evaluate the evolution of the active modes of the small molecules when adsorbed on MOF-74 finding a number of phenomena like the emergence of forbidden bands, the lack of degeneration of some modes, the band splittings and frequency shifts. In particular, we find that the magnitude of these frequency shifts are closely related to the interaction strength of the adsorbate. Furthermore, we realize that these small adsorbates possess some characteristic bands in the high wavenumber region, where the bare MOFs lacks of any relevant IR/Raman fingerprint. Thus, they can be used

to identify the presence and nature of adsorbed molecules or to perform chemical analysis. Finally, we study the variations of the most intense bands of the spectra associated to the typical vibrations of the organic ligands. Although it is difficult to establish quantitative trends, we find distinctive behaviors between weakly bonded systems (Ar and CO_2) and strongly interacting adsorbates (H_2O and NH_3) revealing a remarkable correlation between frequency shifts and adsorbate interaction strength.

Acknowledgement

C.R.M. acknowledges funding from the Spanish MICINN via the Juan de la Cierva-Formación program (ref. FJC2018-036832) and previously from the scholarship program "Oportunidad al Talento" of Fundación ONCE. Spanish MICINN is acknowledged for the funding of a national project (ref. PID2019-111189GB-I00). We thank also C3UPO for the HPC support.

Supporting Information Available

Further structural parameters (S1), Complete spectra of loaded MOFs (S2), Vibrational spectra of isolated adsorbates (S3), Frequency shifts of adsorbed molecules (S4) Frequency shifts of loaded MOFs (S5).

References

(1) Furukawa, H.; Cordova, K. E.; O'Keeffe, M.; Yaghi, O. M. The Chemistry and Applications of Metal-Organic Frameworks. *Science* **2013**, *341*, 1230444.

(2) Kökçam-Demir, U.; Goldman, A.; Esrafili, L.; Gharib, M.; Morsali, A.; Weingart, O.; Janiak, C. Coordinatively Unsaturated Metal Sites (Open Metal Sites) in Metal-Organic Frameworks: Design and Applications. *Chem. Soc. Rev.* **2020**, *49*, 2751–2798.

(3) Rosi, N. L.; Kim, J.; Eddaoudi, M.; Chen, B.; O'Keeffe, M.; Yaghi, O. M. Rod Packings and Metal-Organic Frameworks Constructed from Rod-Shaped Secondary Building Units. *J. Am. Chem. Soc.* **2005**, *127*, 1504–1518.

(4) Britt, D.; Furukawa, H.; Wang, B.; Grant Glover, T.; Yaghi, O. M. Highly Efficient Separation of Carbon Dioxide by a Metal-Organic Framework Replete with Open Metal Sites. *Proc. Natl. Acad. Sci. U.S.A.* **2009**, *106*, 20637–20640.

(5) Wu, H.; Zhou, W.; Yildirim, T. High-Capacity Methane Storage in Metal-Organic Frameworks M_2(dhtp): The Important Role of Open Metal Sites. *J. Am. Chem. Soc.* **2009**, *131*, 4995–5000.

(6) Dietzel, P. D. C.; Besikiotis, V.; Blom, R. Application of Metal–Organic Frameworks with Coordinatively Unsaturated Metal Sites in Storage and Separation of Methane and Carbon Dioxide. *J. Mater. Chem.* **2009**, *19*, 7362–7370.

(7) Grant Glover, T.; Peterson, G. W.; Schindler, B. J.; Britt, D.; Yaghi, O. MOF-74 Building Unit Has a Direct Impact on Toxic Gas Adsorption. *Chem. Eng. Sci.* **2011**, *66*, 163–170.

(8) Bloch, E. D.; Queen, W. L.; Krishna, R.; Zadrozny, J. M.; Brown, C. M.; Long, J. R. Hydrocarbon Separations in a Metal-Organic Framework with Open Iron(II) Coordination Sites. *Science* **2012**, *335*, 1606–1610.

(9) Bae, Y.-S.; Lee, C. Y.; Kim, K. C.; Farha, O. K.; Nickias, P.; Hupp, J. T.; Nguyen, S. T.; Snurr, R. Q. High Propene/Propane Selectivity in Isostructural Metal-Organic Frameworks with High Densities of Open Metal Sites. *Angew. Chem. Int. Ed.* **2012**, *51*, 1857–1860.

(10) Wu, H.; Simmons, J. M.; Srinivas, G.; Zhou, W.; Yildirim, T. Adsorption Sites and Binding Nature of CO_2 in Prototypical Metal-Organic Frameworks: A Combined Neutron Diffraction and First-Principles Study. *J. Phys. Chem. Lett.* **2010**, *1*, 1946–1951.

(11) Poloni, R.; Smit, B.; Neaton, J. B. CO_2 Capture by Metal-Organic Frameworks with van der Waals Density Functionals. *J. Phys. Chem. A* **2012**, *116*, 4957–4964.

(12) Poloni, R.; Lee, K.; Berger, R. F.; Smit, B.; Neaton, J. B. Understanding Trends in CO_2 Adsorption in Metal-Organic Frameworks with Open-Metal Sites. *J. Phys. Chem. Lett.* **2014**, *5*, 861–865.

(13) Queen, W. L.; Hudson, M. R.; Bloch, E. D.; Mason, J. A.; Gonzalez, M. I.; Lee, J. S.; Gygi, D.; Howe, J. D.; Lee, K.; Darwish, T. A.; James, M.; Peterson, V. K.; Teat, S. J.; Smit, B.; Neaton, J. B.; Long, J. R.; Brown, C. M. Comprehensive Study of Carbon Dioxide Adsorption in the Metal-Organic Frameworks M_2(dobdc) (M = Mg, Mn, Fe, Co, Ni, Cu, Zn). *Chem. Sci.* **2014**, *5*, 4569–4581.

(14) Lee, J. S.; Vlaisavljevich, B.; Britt, D. K.; Brown, C. M.; Haranczyk, M.; Neaton, J. B.; Smit, B.; Long, J. R.; Queen, W. L. Understanding Small-Molecule Interactions in Metal–Organic Frameworks: Coupling Experiment with Theory. *Adv. Mater.* **2015**, *27*, 5785–5796.

(15) Vlaisavljevich, B.; Huck, J.; Hulvey, Z.; Lee, K.; Mason, J. A.; Neaton, J. B.; Long, J. R.; Brown, C. M.; Alfé, D.; Michaelides, A.; Smit, B. Performance of van der Waals Corrected Functionals for Guest Adsorption in the M_2(dobdc) Metal-Organic Frameworks. *J. Phys. Chem. A* **2017**, *121*, 4139–4151.

(16) Caskey, S. R.; Wong-Foy, A. G.; Matzger, A. J. Dramatic Tuning of Carbon Dioxide Uptake via Metal Substitution in a Coordination Polymer with Cylindrical Pores. *J. Am. Chem. Soc.* **2008**, *130*, 10870–10871.

(17) Tan, K.; Zuluaga, S.; Gong, Q.; Canepa, P.; Wang, H.; Li, J.; Chabal, Y. J.; Thonhauser, T. Water Reaction Mechanism in Metal Organic Frameworks with Coordinatively Unsaturated Metal Ions: MOF-74. *Chem. Mater.* **2014**, *26*, 6886–6895.

(18) Zuluaga, S.; Fuentes-Fernandez, E. M. A.; Tan, K.; Xu, F.; Li, J.; Chabal, Y. J.; Thonhauser, T. Understanding and Controlling Water Stability of MOF-74. *J. Mater. Chem. A* **2016**, *4*, 5176–5183.

(19) Romero-Muñiz, C.; Paredes-Roibás, D.; López, C.; Hernanz, A.; Gavira-Vallejo, J. M. Assignment of the Raman Spectrum of Benzylic Amide [2] Catenane: Raman Microscopy Experiments and First-Principles Calculations. *J. Phys. Chem. C* **2018**, *122*, 18102–18109.

(20) Romero-Muñiz, C.; Paredes-Roibás, D.; Hernanz, A.; Gavira-Vallejo, J. M. A Comprehensive Study of the Molecular Vibrations in Solid-State Benzylic Amide [2]Catenane. *Phys. Chem. Chem. Phys.* **2019**, *21*, 19538–19547.

(21) Yao, Y.; Nijem, N.; Li, J.; Chabal, Y. J.; Langreth, D. C.; Thonhauser, T. Analyzing the Frequency Shift of Physiadsorbed CO_2 in Metal Organic Framework Materials. *Phys. Rev. B* **2012**, *85*, 064302.

(22) Nijem, N.; Canepa, P.; Kong, L.; Wu, H.; Li, J.; Thonhauser, T.; Chabal, Y. J. Spectroscopic Characterization of van der Waals Interactions in a Metal Organic Framework with Unsaturated Metal Centers: MOF-74–Mg. *J. Phys.: Condens. Matter* **2012**, *24*, 424203.

(23) Kapelewski, M. T.; Geier, S. J.; Hudson, M. R.; Stück, D.; Mason, J. A.; Nelson, J. N.; Xiao, D. J.; Hulvey, Z.; Gilmour, E.; FitzGerald, S. A.; Head-Gordon, M.; Brown, C. M.; Long, J. R. M_2(m-dobdc) (M = Mg, Mn, Fe, Co, Ni) Metal-Organic Frameworks Exhibiting Increased Charge Density and Enhanced H_2 Binding at the Open Metal Sites. *J. Am. Chem. Soc.* **2014**, *136*, 12119–12129.

(24) Tan, K.; Zuluaga, S.; Gong, Q.; Gao, Y.; Nijem, N.; Li, J.; Thonhauser, T.; Chabal, Y. J. Competitive Coadsorption of CO_2 with H_2O, NH_3, SO_2, NO, NO_2, N_2, O_2, and CH_4 in

M-MOF-74 (M = Mg, Co, Ni): The Role of Hydrogen Bonding. *Chem. Mater.* **2015**, *27*, 2203–2217.

(25) Tan, K.; Zuluaga, S.; Wang, H.; Canepa, P.; Soliman, K.; Cure, J.; Li, J.; Thonhauser, T.; Chabal, Y. J. Interaction of Acid Gases SO_2 and NO_2 with Coordinatively Unsaturated Metal Organic Frameworks: M-MOF-74 (M = Zn, Mg, Ni, Co). *Chem. Mater.* **2017**, *29*, 4227–4235.

(26) Ania, C. O.; García-Pérez, E.; Haro, M.; Gutiérrez-Sevillano, J. J.; Valdés-Solís, T.; Parra, J. B.; Calero, S. Understanding Gas-Induced Structural Deformation of ZIF-8. *J. Phys. Chem. Lett.* **2012**, *3*, 1159–1164.

(27) Cohen de Lara, E. Electric Field Effect on Molecules: Relation Between the Orientation of the Molecule with Respect to the Field and the Vibrational Frequency Shift observed in IR Spectra of Molecules Adsorbed in Zeolites. *Phys. Chem. Chem. Phys.* **1999**, *1*, 501–505.

(28) Kresse, G.; Furthmüller, J. Efficient Iterative Schemes for Ab Initio Total-Energy Calculations Using a Plane-Wave Basis Set. *Phys. Rev. B* **1996**, *54*, 11169.

(29) Blöchl, P. E. Projector Augmented-Wave Method. *Phys. Rev. B* **1994**, *50*, 17953.

(30) Kresse, G.; Joubert, D. From Ultrasoft Pseudopotentials to the Projector Augmented-Wave Method. *Phys. Rev. B* **1999**, *59*, 1758.

(31) Perdew, J. P.; Burke, K.; Ernzerhof, M. Generalized Gradient Approximation Made Simple. *Phys. Rev. Lett.* **1996**, *77*, 3865.

(32) Grimme, S.; Antony, J.; Ehrlich, S.; Krieg, H. A Consistent and Accurate Ab Initio Parametrization of Density Functional Dispersion Correction (DFT-D) for the 94 Elements H-Pu. *J. Chem. Phys.* **2010**, *132*, 154104.

(33) Rana, M. K.; Koh, H. S.; Hwang, J.; Siegel, D. J. Comparing van der Waals Density Functionals for CO_2 Adsorption in Metal Organic Frameworks. *J. Phys. Chem. C* **2012**, *116*, 16957–16968.

(34) Monkhorst, H. J.; Pack, J. D. Special Points for Brillouin-Zone Integrations. *Phys. Rev. B* **1976**, *13*, 5188.

(35) Gonzalez, M. I.; Mason, J. A.; Bloch, E. D.; Teat, S. J.; Gagnon, K. J.; Morrison, G. Y.; Queen, W. L.; Long, J. R. Structural Characterization of Framework–Gas Interactions in the Metal–Organic Framework Co_2(dobdc) by in Situ Single-Crystal X-ray Diffraction. *Chem. Sci.* **2017**, *8*, 4387–4398.

(36) Wilson Jr., E. B.; Decius, J. D.; Cross, P. C. *Molecular Vibrations*; McGraw-Hill, 1955.

(37) Woodward, L. A. *Introduction to the Theory of Molecular Vibrations and Vibrational Spectroscopy*; Oxford University Press, 1972.

(38) Long, D. A. *The Raman Effect: A Unified Treatment of the Theory of Raman Scattering by Molecules*; John Wiley & Sons, 2002.

(39) Giannozzi, P.; Baroni, S. Vibrational and Dielectric Properties of C_{60} from Density-Functional Perturbation Theory. *J. Chem. Phys.* **1994**, *100*, 8537–8539.

(40) Baroni, S.; de Gironcoli, S.; Dal Corso, A.; Giannozzi, P. Phonons and Related Crystal Properties from Density-Functional Perturbation Theory. *Rev. Mod. Phys.* **2001**, *73*, 515–562.

(41) Gajdoš, M.; Hummer, K.; Kresse, G.; Furthmüller, J.; Bechstedt, F. Linear Optical Properties in the Projector-Augmented Wave Methodology. *Phys. Rev. B* **2006**, *73*, 045112.

(42) Valenzano, L.; Civalleri, B.; Sillar, K.; Sauer, J. Heats of Adsorption of CO and CO_2 in

Metal-Organic Frameworks: Quantum Mechanical Study of CPO-27-M (M = Mg, Ni, Zn). *J. Phys. Chem. C* **2011**, *115*, 21777–21784.

(43) Koh, H. S.; Rana, M. K.; Hwang, J.; Siegel, D. J. Thermodynamic Screening of Metal-Substituted MOFs for Carbon Capture. *Phys. Chem. Chem. Phys.* **2013**, *15*, 4573–4581.

(44) Canepa, P.; Arter, C. A.; Conwill, E. M.; Johnson, D. H.; Shoemaker, B. A.; Soliman, K. Z.; Thonhauser, T. High-Throughput Screening of Small-Molecule Adsorption in MOF. *J. Mater. Chem. A* **2013**, *1*, 13597–13604.

(45) Lee, K.; Howe, J. D.; Lin, L.-C.; Smit, B.; Neaton, J. B. Small-Molecule Adsorption in Open-Site Metal–Organic Frameworks: A Systematic Density Functional Theory Study for Rational Design. *Chem. Mater.* **2015**, *27*, 668–678.

(46) Zhou, W.; Wu, H.; Yildirim, T. Enhanced H_2 Adsorption in Isostructural Metal-Organic Frameworks with Open Metal Sites: Strong Dependence of the Binding Strength on Metal Ions. *J. Am. Chem. Soc.* **2008**, *130*, 15268–15269.

(47) Queen, W. L.; Brown, C. M.; Britt, D. K.; Zajdel, P.; Hudson, M. R.; Yaghi, O. M. Site-Specific CO_2 Adsorption and Zero Thermal Expansion in an Anisotropic Pore Network. *J. Phys. Chem. C* **2011**, *115*, 24915–24919.

(48) Dietzel, P. D. C.; Panella, B.; Hirscher, M.; Blom, R.; Fjellvåg, H. Hydrogen Adsorption in a Nickel Based Coordination Polymer with Open Metal Sites in the Cylindrical Cavities of the Desolvated Framework. *Chem. Commun.* **2006**, 959–961.

(49) Dietzel, P. D. C.; Morita, Y.; Blom, R.; Fjellvåg, H. An In Situ High-Temperature Single-Crystal Investigation of a Dehydrated Metal-Organic Framework Compound and Field-Induced Magnetization of One-Dimensional Metal–Oxygen Chains. *Angew. Chem. Int. Ed.* **2005**, *44*, 6354–6358.

(50) Park, J.; Kim, H.; Han, S. S.; Jung, Y. Tuning Metal-Organic Frameworks with Open-Metal Sites and Its Origin for Enhancing CO_2 Affinity by Metal Substitution. *J. Phys. Chem. Lett.* **2012**, *3*, 826–829.

(51) Canepa, P.; Nijem, N.; Chabal, Y. J.; Thonhauser, T. Diffusion of Small Molecules in Metal Organic Framework Materials. *Phys. Rev. Lett.* **2013**, *110*, 026102.

(52) Marti, R. M.; Howe, J. D.; Morelock, C. R.; Conradi, M. S.; Walton, K. S.; Sholl, D. S.; Hayes, S. E. CO_2 Dynamics in Pure and Mixed-Metal MOFs with Open Metal Sites. *J. Phys. Chem. C* **2017**, *121*, 25778–25787.

(53) Valenzano, L.; Civalleri, B.; Chavan, S.; Palomino, G. T.; Areán, C. O.; Bordiga, S. Computational and Experimental Studies on the Adsorption of CO, N_2, and CO_2 on Mg-MOF-74. *J. Phys. Chem. C* **2010**, *114*, 11185–11191.

(54) Vazhappilly, T.; Ghanty, T. K.; Jagatap, B. N. Computational Modeling of Adsorption of Xe and Kr in M-MOF-74 Metal Organic Frame Works with Different Metal Atoms. *J. Phys. Chem. C* **2016**, *120*, 10968–10974.

(55) Maslowsky, E. J. *Vibrational Spectra of Organometallics: Theoretical and Experimental data*; John Wiley & Sons, 2019.

(56) Johnson, M. K.; Powell, D. B.; Cannon, R. D. Vibrational Spectra of Carboxylato Complexes-I. Infrared and Raman Spectra of Beryllium(II) Acetate and Formate and of Zinc(II) Acetate and Zinc(II) Acetate Dihydrate. *Spectrochim. Acta, Part A* **1981**, *37*, 899–904.

(57) Johnson, M. K.; Powell, D. B.; Cannon, R. D. Vibrational Spectra of Carboxylato Complexes-II. Some Oxo-Tetranuclear Complexes. *Spectrochim. Acta, Part A* **1982**, *38*, 125–131.

(58) Colthup, N. B.; Daly, L. H.; Wiberley, S. E. *Introduction to Infrared and Raman Spectroscopy*, 3rd ed.; Academic Press, 1990.

(59) Herzberg, G. *Molecular Spectra and Molecular Structure: II Infrared and Raman Spectra of Polyatomic Molecules*; Van Nostrand, 1945.

(60) Nijem, N.; Veyan, J.-F.; Kong, L.; Wu, H.; Zhao, Y.; Li, J.; Langreth, D. C.; Chabal, Y. J. Molecular Hydrogen "Pairing" Interaction in a Metal Organic Framework System with Unsaturated Metal Centers (MOF-74). *J. Am. Chem. Soc.* **2010**, *132*, 14834–14848.

(61) Serre, C.; Bourrelly, S.; Vimont, A.; Ramsahye, N. A.; Maurin, G.; Llewellyn, P. L.; Daturi, M.; Filinchuk, Y.; Leynaud, O.; Barnes, P.; Férey, G. An Explanation for the Very Large Breathing Effect of a Metal-Organic Framework during CO_2 Adsorption. *Adv. Mater.* **2007**, *19*, 2246–2251.

(62) FitzGerald, S. A.; Schloss, J. M.; Pierce, C. J.; Thompson, B.; Rowsell, J. L. C.; Yu, K.; Schmidt, J. R. Insights into the Anomalous Vibrational Frequency Shifts of CO_2 Adsorbed to Metal Sites in Microporous Frameworks. *J. Phys. Chem. C* **2015**, *119*, 5293–5300.

(63) Borfecchia, E.; Maurelli, S.; Gianolio, D.; Groppo, E.; Chiesa, M.; Bonino, F.; Lamberti, C. Insights into Adsorption of NH_3 on HKUST-1 Metal–Organic Framework: A Multitechnique Approach. *J. Phys. Chem C* **2012**, *116*, 19839–19850.

(64) Saha, D.; Deng, S. Ammonia Adsorption and its Effects on Framework Stability of MOF-5 and MOF-177. *J. Colloid Interface Sci.* **2010**, *348*, 615–620.

(65) Strauss, I.; Mundstock, A.; Hinrichs, D.; Himstedt, R.; Knebel, A.; Reinhardt, C.; Dorfs, D.; Caro, J. The Interaction of Guest Molecules with Co-MOF-74: A Vis/NIR and Raman Approach. *Angew. Chem. Int. Ed.* **2018**, *57*, 7434–7439.

Graphical TOC Entry